Methodology and Case Studies of Signal-in-Space Error Calculation
Top-down Meets Bottom-up

Grace Xingxin Gao*, Haochen Tang*, Juan Blanch*,
Jiyun Lee+, Todd Walter* and Per Enge*
* Stanford University, USA
+ KAIST, Korea

BIOGRAPHY

Grace Xingxin Gao is a research associate in the GPS lab of Stanford University. She received her B.S. degree in Mechanical Engineering in 2001 and her M.S. degree in Electrical Engineering in 2003, both at Tsinghua University, China. She obtained her Ph.D. degree in Electrical Engineering at Stanford University in 2008. Her current research interests include GNSS signal and code structures, GNSS receiver architectures, interference mitigation and GNSS signal error analysis. She received the Institute of Navigation (ION) Early Achievement Award in 2008.

Haochen Tang is currently a Ph.D student in the Dept. of Aeronautics and Astronautics working in the GPS Lab of Stanford University. He received his bachelor degree in mechanical engineering from Tsinghua University in Beijing, China in 2006 and master degree of mechanical and aerospace engineering from Illinois Institute of Technology in Chicago, IL in 2009. His research interests are algorithm development and software simulation for GNSS applications in civil aviation.

Juan Blanch received a Ph.D. in Aeronautics and Astronautics in December 2003 from Stanford University, for his work on ionospheric estimation for the Wide Area Augmentation System (WAAS). He has continued as a Research Associate in the Stanford GPS laboratory, where he is currently developing algorithms for civil aviation navigation integrity.

Jiyun Lee is an assistant professor at KAIST in Korea. She received her B.S. degree from Yonsei University, Korea and her M.S. degree in Aerospace Engineering and Science from the University of Colorado at Boulder. She joined the Stanford GPS laboratory in 2000, received her Ph.D. degree from the Aeronautics and Astronautics department in 2005, and continued working as a Post-Doctoral researcher in the GPS laboratory. Her Ph.D. thesis focused on the development of a GPS-based aircraft landing system.

Todd Walter is a senior research engineer in the Department of Aeronautics and Astronautics at Stanford University. He received his Ph.D. from Stanford and is currently working on the Wide Area Augmentation System (WAAS), defining future architectures to provide aircraft guidance, and working with the FAA and GPS-Wing on assuring integrity on GPS-III. Key early contributions include: prototype development proving the feasibility of WAAS, significant contribution to WAAS MOPS, and design of ionospheric algorithms for WAAS. He is a fellow of the Institute of Navigation.

Per Enge is a Professor of Aeronautics and Astronautics at Stanford University, where he is the Kleiner-Perkins, Mayfield, Sequoia Capital Professor in the School of Engineering. He directs the GPS Research Laboratory, which develops satellite navigation systems based on the Global Positioning System (GPS). He has been involved in the development of WAAS and LAAS for the FAA. Per has received the Kepler, Thurlow and Burka Awards from the ION for his work. He is also a Fellow of the ION and the Institute of Electrical and Electronics Engineers (IEEE). He received his PhD from the University of Illinois in 1983.

ABSTRACT

Signal in space (SIS) errors are a major error source for the Global Positioning System (GPS). They are defined as any errors related to satellite transmission, mainly satellite position and clock errors. A better understanding and characterization of the signal in space errors are essential for GPS integrity, because the SIS errors are a metric to determine satellite outages or failures. The statistics of the SIS errors are an important factor to monitor the system performance in terms of integrity.

We present two methods to calculate SIS errors. One is called top-down, which is based on high data rate dual frequency measurements obtained from the Wide Area Augmentation System (WAAS) or the National Satellite Test Bed (NSTB) networks. The SIS errors of a satellite are obtained by stripping off all non-SIS errors from the total pseudo-range error. We apply our algorithm to L1/L2 measurements now as an intermediate step to migrate to L1/L5 measurements when L5 signals are available in the future. The other way of characterizing SIS errors is the bottom-up method, which builds up the SIS errors by summing the satellite position errors and satellite clock errors, etc. The satellite position and clock errors are calculated by differentiating broadcast and precise ephemerides obtained from the International GNSS Service (IGS) network and the National Geospatial Intelligence (NGA) network, respectively. The top-down and bottom-up methods well complement each other.

In the second part of the paper, we apply the top-down and bottom-up methods to two actual satellite outages from 2007. The results show that the two methods match well no matter whether a satellite is faulted or not. The discrepancies of the two methods are currently within +/- 4 meters and are independent of the carrier smoothing filter length.

INTRODUCTION

Integrity of the Global Navigation Satellite System (GNSS) is essential for a wide range of applications, from existing navigation for land vehicles, ships and aircraft to future aircraft landing. To maintain the integrity of the systems, it is desirable to monitor the satellite performance; in other words, to measure the errors associated with the satellites, defined as signal in space (SIS) errors.

Figure 1 shows an overview of the major GPS signal error sources. We categorize the errors into three types.

- First, the errors related to the receiver and the local environment, mainly the receiver clock error and the multipath error.
- Second, the propagation errors (including the ionosphere delay and the troposphere delay).
- Third, the signal-in-space errors, which are the errors related to the satellite transmission.
  The main contributions of the signal-in-space errors are the satellite position error and the satellite clock error. In other words, the true satellite position and clock are off from the satellite position and clock being broadcast via navigation messages. In addition, signal in space errors also include satellite antenna phase and group delay variations, code-carrier incoherence, signal deformation, relativistic correction errors and any inter-signal errors included in the satellites [1].

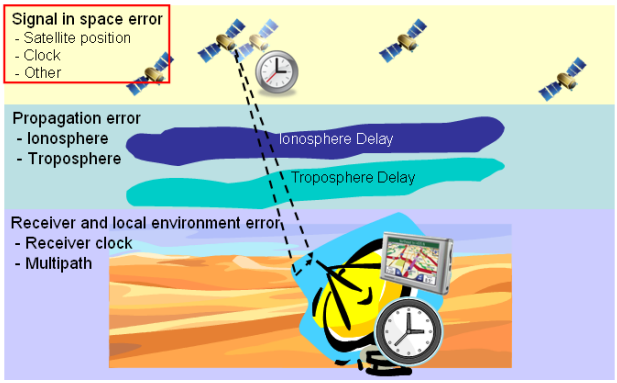

Figure 1. Overview of major GPS signal errors

Characterization and estimation of the signal-in-space errors are essential for GPS integrity. SIS errors are used to identify satellite failures. A major service failure is declared if SIS errors go beyond 4.42*User Range Accuracy (URA). The statistics of the SIS errors are also useful for evaluating URA as a valid indicator of performance.

So far, the signal in space errors in the Global Positioning System (GPS) have been monitored by the FAA tech center through the National Satellite Test Bed (NSTB) and Wide Area Augmentation System (WAAS), and are published offline in the GPS Performance Analysis (PAN) report [2]. The GPS PAN report shows that the current monitoring system provides continuous signal in space error evaluation based on the L1 frequency only.

Although the GPS SIS errors have been well studied [3-6], a better understanding of the SIS errors is required. Most of the prior work used data with a data rate of 15 minutes. However, anomalies could be much shorter, even shorter than 6 seconds. In this paper, we present top-down versus bottom-up approaches. The top-down approach has a high data rate of 1 Hz and thus can detect fast anomalies.

TOP-DOWN METHODOLOGY

We present two approaches to characterize signal in space errors. The first approach is the “top-down” method, which strips off all the non-SIS errors from the total pseudo-range error, namely the ionosphere and troposphere delays, the multipath error, and the receiver clock error.

A. Data Source

We use data from the Wide Area Augmentation System (WAAS) and National Satellite Test Bed (NSTB) Networks shown in Figure 2 [7]. The WAAS network has 38 WAAS stations in North America, with 3 receivers per

station. The 114 receivers output pseudo-range measurements and navigation messages at a data update rate of 1 Hz. The advantages of WAAS/NSTB networks are the fast data rate and the receiver redundancy. The output data every 1 sec sufficiently captures short satellite outages. The redundancy of 3 receivers per station can eliminate receiver glitches. In addition to the advantages, the WAAS/NSTB networks have some constraints. First, the coverage of the network is the Conterminous North America only. Since the receiver network does not have the full world coverage, only outages of satellites in view of the receivers can be detected. Moreover, only the recent weeks of the WAAS/NSTB data are readily available on the website. It is not straightforward to retrieve past WAAS/NSTB data. It is necessary to contact the FAA Tech Center to get data manually retrieved.

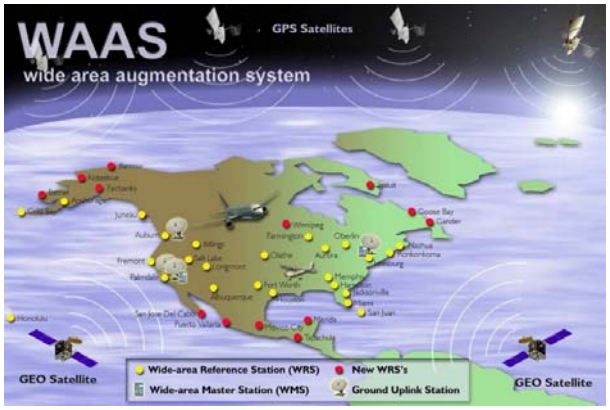

Figure 2. 38 WAAS stations

B. Algorithm

The top-down algorithm forms dual-frequency ionosphere-free combination measurements, calculates the troposphere delay, smoothes multipath errors, estimates the receiver clock bias, and then strips off all the non-SIS errors from the total pseudo-range errors. The total pseudo-range error is obtained by using receivers at surveyed locations.

We the form dual-frequency ionosphere-free combination of L1 and L2 measurements to eliminate ionosphere delay [11].

$$\rho_{IF} = \frac{f_{L1}^2}{f_{L1}^2 - f_{L2}^2}\rho_{L1} - \frac{f_{L2}^2}{f_{L1}^2 - f_{L2}^2}\rho_{L2}, \qquad \text{eq. (1)}$$
$$\Phi_{IF} = \frac{f_{L1}^2}{f_{L1}^2 - f_{L2}^2}\Phi_{L1} - \frac{f_{L2}^2}{f_{L1}^2 - f_{L2}^2}\Phi_{L2},$$

where ρ_{IF}, ρ_{L1}, and ρ_{L2} are the code measurements of ionosphere-free combination, L1 frequency band and L2 band, respectively; Φ_{IF}, Φ_{L1}, and Φ_{L2} are the carrier measurements of the ionosphere-free combination, L1 frequency band, and L2 band, respectively; f_{L1} is the L1 band center frequency, or 1575.42 MHz; and f_{L2} is the L2 band center frequency, which is 1227.60 MHz. Although the dual-frequency ionosphere-free combination efficiently eliminates ionosphere delay, it increases the noise level.

Troposphere delay is estimated by the model defined in the WAAS MOPS, which is a vertical troposphere model adjusted by a mapping function of satellite elevation [8].

$$\sigma_{i,tropo} = \sigma_{TVE} \cdot m(El_i), \qquad \text{eq. (2)}$$

where $\sigma_{i,tropo}$ is the troposphere delay for satellite i, σ_{TVE} is the troposphere vertical error and $m(El_i)$ is the mapping function for satellite i, which is dependent on the satellite elevation.

The multipath error is mitigated by carrier smoothing as shown in the following equations [9].

$$\bar{\rho}(t_i) = \frac{1}{M}\rho(t_i) + \frac{(M-1)}{M}[\bar{\rho}(t_{i-1}) + (\Phi(t_i) - \Phi(t_{i-1}))], \qquad \text{eq. (3)}$$
$$\bar{\rho}(t_1) = \rho(t_1),$$

where $\rho(t_i)$ and $\Phi(t_i)$ are the pseudo-range and carrier measurements at time t_i, respectively, $\bar{\rho}(t_i)$ is the smoothed pseudo-range measurements, and M is the filter length of the carrier smoothing.

After stripping off the ionosphere, troposphere and multipath errors, only the receiver clock error and signal in space errors remain. As the last step of the top-down method, we need to calculate the receiver clock error. The receiver clock error is a common bias for pseudo-ranges of all satellites in view. We assume that the probability of signal in space errors among healthy satellites is identical and independent with zero mean. This assumption will be verified by the case study results. The receiver clock bias is calculated by averaging the remaining errors over all observed healthy satellites.

BOTTOM-UP METHODOLOGY

The other approach is the "bottom-up" method. Different from stripping off the non-SIS error, the "bottom-up" method approximates the SIS errors with the satellite position errors and clock errors, and builds up the SIS errors by summing the satellite position and clock errors.

A. Data Source

The satellite position and clock errors are calculated by differencing the true ephemeris with the broadcast ephemerides.

The broadcast ephemerides are obtained from the International GNSS Service (IGS) network [10]. The IGS

network has over 350 receivers all over the world as shown in Figure 3. They output both the range measurements and the ephemeris information in RINEX format. The ephemeris information is updated every 2 hours.

The National Geospatial Intelligence Agency (NGA) network provides the post-processed truth ephemerides [11]. It has 12 stations all over the world as shown in Figure 4, fewer than those of the IGS network. The stations output the satellite position and the clock, plus the change rate of position and clock every 15 minutes.

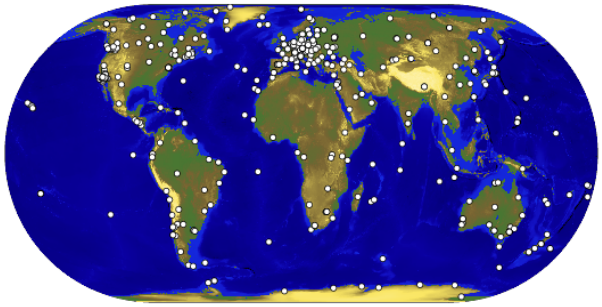

Figure 3. 364 IGS stations all over the world

Figure 4. 12 NGA stations all over the world

Both the IGS and NGA networks have full worldwide coverage. They can calculate SIS errors of all satellites continuously. No matter where the satellites are during outage, there are always receivers in the IGS and NGA networks that can detect the outage. Recent years of data are available on the IGS and NGA websites, which makes it easy to retrieve old data and calculate satellite SIS errors in the past. However, the slow network update rate is the main disadvantage. The data rates of every 2 hours for broadcast ephemerides from IGS and every 15 minutes for NGA are not sufficient to capture outages less than 15 minutes.

B. Algorithm

We determine the difference between the broadcast ephemerides calculated from the IGS network and the precise ephemerides provided by the NGA network. Figure 5 shows the flow chart of the bottom-up method. The IGS and NGA networks do not provide ephemerides information at the same time stamps. We need to propagate the IGS ephemerides to the same times as those of NGA for fair comparison. We first choose a proper broadcast ephemeris with the most recent TTOM (Transmission Time of Message) compared to the time of the truth. We then propagate the broadcast satellite positions to the time of the truth based on Kepler law [9]. The broadcast satellite clock error is also propagated based on the clock rate, the clock acceleration rate and the time difference. After the time is aligned, we calculate the difference between the propagated broadcast ephemerides and the truth. Finally the ephemeris errors are projected onto the line-of-sight of the satellite and a certain receiver on Earth.

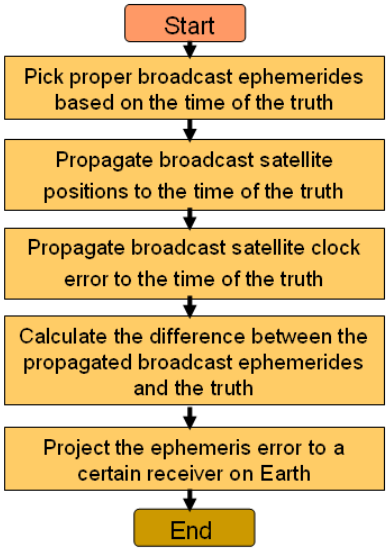

Figure 5. Flow chart of bottom-up method

TOP-DOWN VERSUS BOTTOM-UP

	Top-down	Bottom-up
Data Source	WAAS & NSTB	IGS & NGA
Control of data source	Yes	No
Data update rate	High, every 1 sec	Low, 15 min
Depend on post-processed truth	No	Yes
Include all SIS errors	Yes	No
Receiver glitches	No for WAAS	Yes
Remove all non SIS errors	No	Yes
Receiver coverage	Limited (North America)	Worldwide, but not even
Data availability	Difficult to retrieve past data	Available

Table 1. Comparison between top-down and bottom-up methods

Both top-down and bottom-up approaches have advantages and disadvantages. The top-down approach

includes all SIS errors, but may not exclude all the non-SIS errors. However, the bottom-up approach includes neither any non-SIS errors nor the complete list of SIS errors. Table 1 summarizes the pros and cons of the top-down methodology versus the bottom-up. The green cells represent the advantages, and the red ones show the disadvantages. The two methods complement each other.

The top-down method uses data from the WAAS and NSTB networks while the data sources of the bottom-up method are IGS and NGA. The WAAS/NSTBs network have a data update rate as fast as every 1 sec. It can capture the fast appearance of the ephemeris errors. The FAA has control of all the receivers in the WAAS/NSTB networks. The three WAAS receivers per station provide redundancies to remove any receiver outliers. However, the FAA techical center website has only the recent few weeks of data available, so it is inconvenient to retrieve the past data. Also, the WAAS/NSTB network is in North America, so it doesn't have world-wide coverage. In comparison, the IGS and NGA networks for the bottom-up method have receivers all over the world. No matter when a satellite outage happens, there are always receivers within the IGS and the NGA networks capturing the outage. The data of recent years rather than weeks are available on the IGS/NGA websites. However, FAA doesn't have control of the receiver networks. There are no receiver redundancies and thus the receiver glitches are not easy to identify and remove. The data update rate is low, every 15 minutes for NGA precise ephemerides and every 2 hours for IGS broadcast ephemerides, which makes it unlikely to capture satellite outages shorter than 15 minutes. The bottom-up method is dependent on the post-processed truth. Although it excludes all the non-SIS errors, it only uses the satellite position and clock errors to approximate the total SIS errors. The top-down method does include all the SIS errors, but may not remove all the non SIS errors due to the non SIS error residuals. Both top-down and bottom-up methods have pros and cons. Fortunately, the two methods complement each other well.

CASE STUDIES

In this section, we will use two real satellite outages in 2007 as case studies to illustrate the top-down and bottom-up methodologies.

The two satellite outages in 2007 are shown in Table 2. One is a planned satellite position outage of PRN 10 on Day 39 of Year 2007; the other one is an unplanned clock outage of PRN 07 on Day 229 of Year 2007.

	PRN 10, Day 39 of Year 2007	**PRN 07, Day 229 of Year 2007**
Planned outage?	Yes	No
Outage type	Satellite position	Satellite clock
Site investigated	Atlantic City, NJ	Arcata, CA

Table 2. Case studies of two outages in 2007

A. PRN 10 on Day 39 of Year 2007

The first case is PRN 10 on Day 39 of 2007. The worst projected ephemeris error is calculated by the bottom-up method. We project the ephemeris error to a receiver grid 1 degree apart covering the whole globe and pick the worst one. As shown in Figures 6 and 7, this outage is a planned outage, as the satellite was already set unhealthy before the large error occurs. The worst projected ephemeris error is larger than 2000 meters, dramatically beyond 4.42 times the URA value.

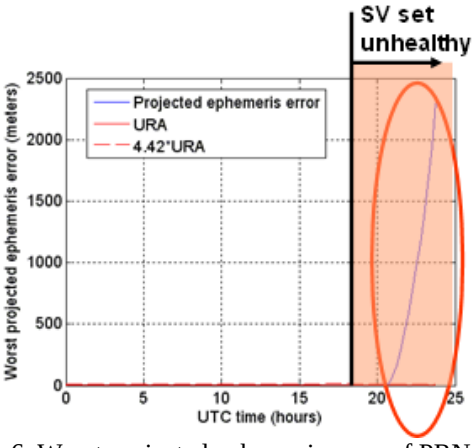

Figure 6. Worst projected ephemeris error of PRN 10 on Day 39, 2007

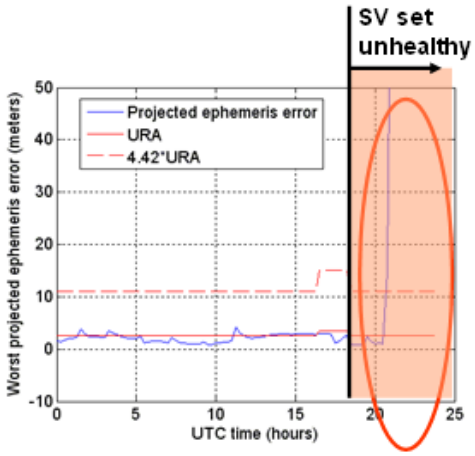

Figure 7. Worst projected ephemeris error of PRN 10 on Day 39, 2007, zoomed in

Figure 9 shows the ground track of PRN 10, where the red part of the curve shows the period when the outage happened. The receivers on the east coast of the US could

observe this outage on Day 39. We pick Atlantic City in New Jersey as the site of investigation.

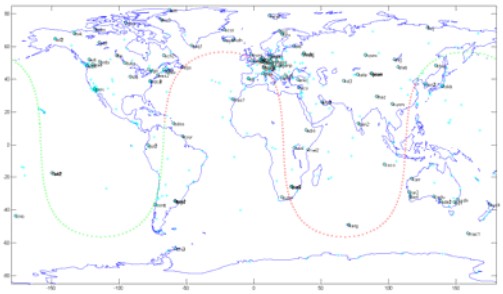

Figure 9. Ground track of PRN 10 on Day 39-40 of Year 2007

Figure 10 shows a comparison of the SIS errors projected at Atlantic City, NJ using the top-down and bottom-up methods. The two methods match very well in both time periods when the satellite behaved normally and when there was an outage.

Figure 11 shows the discrepancies between the top-down and the bottom up results. Again, the discrepancies are consistent no matter whether the error is large or not. Recall that when calculating the receiver clock error using the top-down method, we assume that the SIS errors across different satellites are uncorrelated. In other words, there is no SIS bias across satellites. This assumption is verified by the fact that the mean discrepancy value is about zero as shown in Figure 11.

The discrepancies are bounded within +/- 4 meters. This result is based on 100-sec carrier smoothing for the top-down calculation.

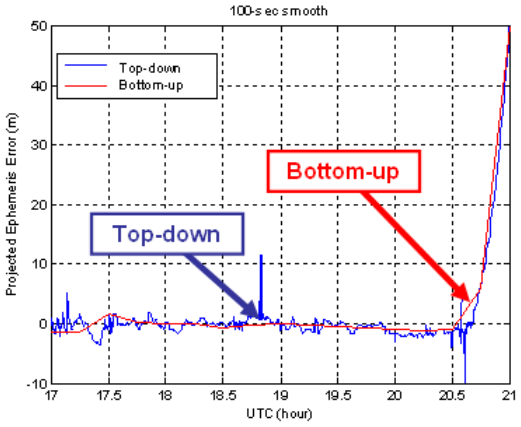

Figure 10. SIS errors of PRN 10 projected at Atlantic City, NJ, Day 39 of Year 2007, with 100-sec carrier smoothing for the top-down method

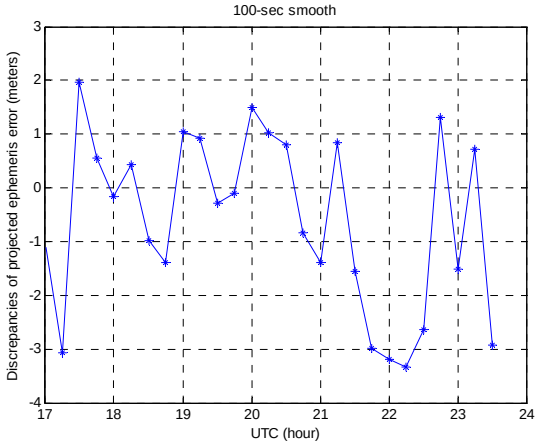

Figure 11. Discrepancies of top-down and bottom-up methods in calculating SIS errors of PRN 10 projected at Atlantic City, NJ, Day 39 of Year 2007, with 100-sec carrier smoothing for the top-down method

We also use a longer carrier smoothing window to examine the effect of the carrier-smoothing filter length, or to see if we can reduce the discrepancies of the two methods. Figure 12 shows the result of 15-minutes of smoothing for the top-down calculation. The smoothing length of 15 minutes is chosen because the NGA network updates the data every 15 minutes. Again, the two methodologies match well for both normal and abnormal periods.

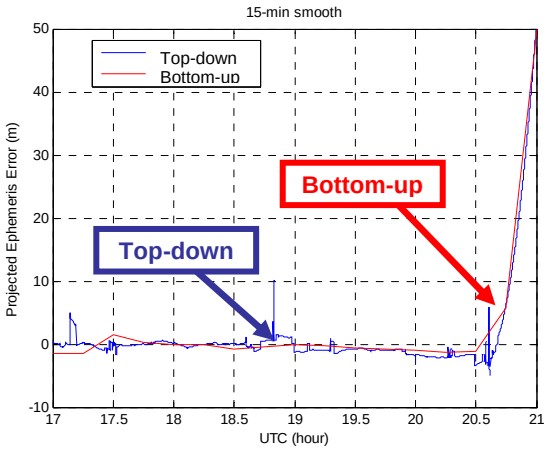

Figure 12. SIS errors of PRN 10 projected at Atlantic City, NJ, Day 39 of Year 2007, with 15-min carrier smoothing for the top-down method

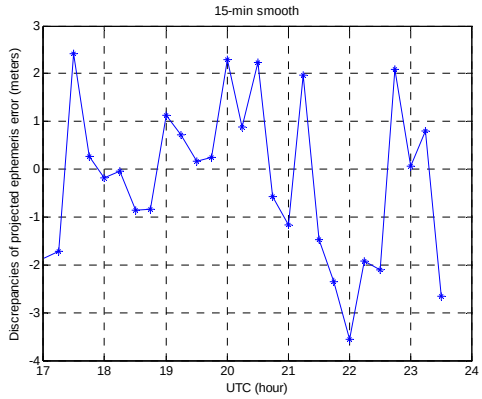

Figure 13. Discrepancies of top-down and bottom-up methods in calculating SIS errors of PRN 10 projected at Atlantic City, NJ, Day 39 of Year 2007, with 15-min carrier smoothing for the top-down method

The discrepancies are consistent over the whole time investigated as shown in Figure 13. However, they are still within +/-4 meters. The longer smoothing time of 15 minutes does not narrow the gap between the top-down and bottom-up methods compared to 100-sec smoothing. This is because we have no knowledge about how the NGA network updates their data every 15 minutes. We do not know if they apply any averaging or smoothing over the time period of 15 minutes, or simply perform sampling every 15 minutes.

B. PRN 07 on Day 229 of Year 2007

The second case study is an anomaly of PRN 07 on Day 229 of Year 2007. Different from the first case study, this anomaly is due to the satellite clock error, not the satellite position error. And it is an unplanned outage, or an anomaly. Figure 14 shows the worst projected ephemeris error including both the satellite position and clock errors.

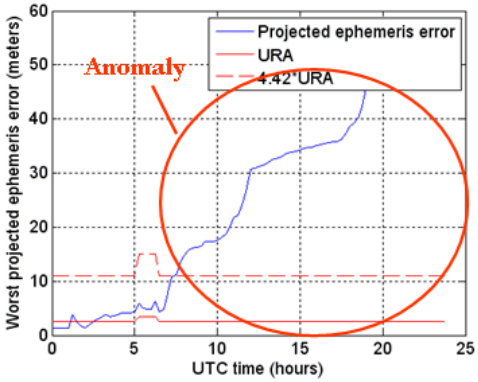

Figure 14. Worst projected ephemeris error of PRN 07 on Day 229, 2007

The ground track of this satellite is shown in Figure 15. Receivers on the west coast can observe this anomaly. We investigate the site of Arcata in California.

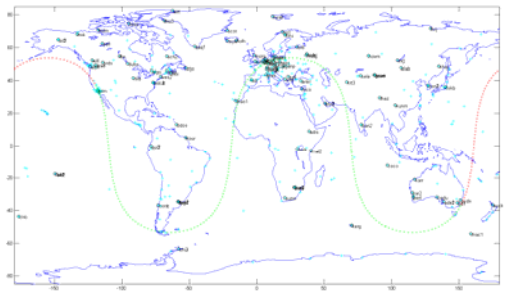

Figure 15. Ground track of PRN 07 on Day 229 of Year 2007

The blue curve in Figure 16 shows the bottom-up result for the SIS errors, and the red curve uses the top-down approach with 100 sec smoothing. In this case, the top-down and bottom-up methods again match very well no matter whether there is an anomaly.

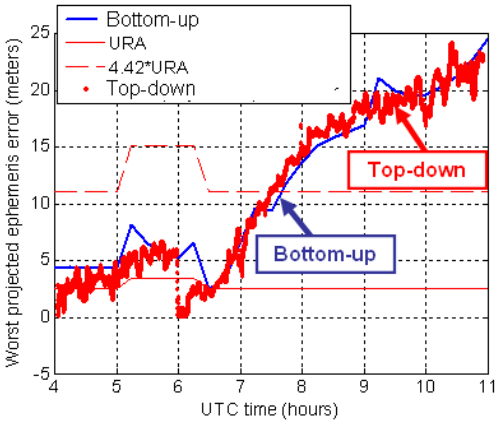

Figure 16. SIS errors of PRN 07 projected at Arcata, CA, Day 229 of Year 2007, with 100-sec carrier smoothing for the top-down method

The discrepancies of the two methods are also bounded within +/-4 meters as shown in Figure 17.

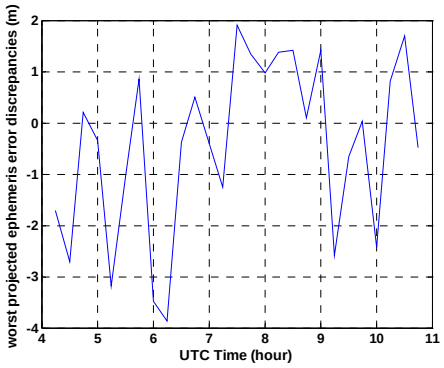

Figure 17. Discrepancies of top-down and bottom-up methods in calculating SIS errors of PRN 07 projected at Arcata, CA, Day 229 of Year 2007, with 100-sec carrier smoothing for the top-down method

There are many reasons for the discrepancies, which are categorized into two types: errors from the top-down method and errors from the bottom-up method. For the top-down method, the dual-frequency ionosphere-free combination eliminates the ionosphere delay, but increases the noise floor. There can be error residuals of troposphere estimate based on the WAAS MOPS model, multipath, receiver clock, and thermal noise. Inaccuracies in precise ephemerides and incorrect choice of active broadcast ephemeris can cause the bottom-up calculation to be off. The inaccuracy of the bottom-up method also comes from not including other error sources, for example, code-carrier incoherence, signal deformation, inter-signal errors, satellite antenna phase center variation, satellite antenna group delay center variation, relativistic correction errors, etc.

The gap of +/- 4 meters shown in this section is a starting point. Our near-term goal is to better estimate the SIS errors and to narrow the gap between the top-down and bottom-up methods to less than 1 meter.

CONCLUSION

Two methodologies for characterizing SIS errors are presented in this paper, namely top-down and bottom-up. The two methods well complement each other. By using both methods, we can capture all satellite outages at anytime including outages shorter than 15 minutes.

Two cases of real satellite outages in 2007 are studied to illustrate the effectiveness of using both top-down and bottom-up methods. The case study results show that the two methods match well no matter whether the error is large or not. The discrepancies are bounded within +/- 4 meters as our starting point. Our future work would include narrowing the discrepancies down to less than 1 meter.

ACKNOWLEDGMENTS

The authors gratefully acknowledge the support of the Federal Aviation Administration under Cooperative Agreement 08-G-007. This paper contains the personal comments and beliefs of the authors, and does not necessarily represent the opinion of any other person or organization.

We would also like to thank Tom McHugh from the William J. Hughes FAA Technical Center for providing the NSTB data of 2007.

REFERENCES

[1]. T. Walter, J. Blanch and P. Enge, “Evaluation of Signal in Space Error Bounds to Support Aviation Integrity”, ION GNSS 2009, Savannah GA

[2]. GPS Performance Analysis (PAN) report, http://www.nstb.tc.faa.gov/reports/PAN64_0109.pdf

[3]. F. Van Grass. “GPS Clock and Orbit Error Distributions”, GNSS Evolutionary Architecture Study (GEAS) meeting, February 2009, Los Angeles CA

[4]. K. Kovach, J. Berg and V. Lin, “Investigation of Upload Anomalies Affecting IIR Satellites in October 2007”, ION GNSS 2008, Savannah GA

[5]. D. L. M. Warren and J. F. Raquet, “Broadcast vs. precise GPS ephemerides: a historical perspective”, GPS Solutions, 2004

[6]. D. Jefferson and Y. Bar-Sever, “Accuracy and consistency of broadcast GPS ephemeris data”, ION GNSS 2000

[7] WAAS/NSTB data download, http://www.nstb.tc.faa.gov/

[8] Wide Area Augmentation System Minimum Operational Performance Standards (WAAS MOPS)

[9] Pratap Misra and Per Enge, Global Positioning System: Signals, Measurements, and Performance Second Edition (2006), Ganga-Jamuna Press

[10] International GNSS Service (IGS) network, http://igscb.jpl.nasa.gov/

[11] National Geospatial Intelligence (NGA) network, http://earth-info.nga.mil/GandG/sathtml/ephemeris.html